

# DEEPTYPE: Refining Indirect Call Targets with Strong Multi-layer Type Analysis

Tianrou Xia  
Pennsylvania State University

Hong Hu  
Pennsylvania State University

Dinghao Wu  
Pennsylvania State University

## Abstract

Indirect calls, while facilitating dynamic execution characteristics in C and C++ programs, impose challenges on precise construction of the control-flow graphs (CFG). This hinders effective program analyses for bug detection (e.g., fuzzing) and program protection (e.g., control-flow integrity). Solutions using data-tracking and type-based analysis are proposed for identifying indirect call targets, but are either time-consuming or imprecise for obtaining the analysis results. Multi-layer type analysis (MLTA), as the state-of-the-art approach, upgrades type-based analysis by leveraging multi-layer type hierarchy, but their solution to dealing with the information flow between multi-layer types introduces false positives. In this paper, we propose strong multi-layer type analysis (SMLTA) and implement the prototype, DEEPTYPE, to further refine indirect call targets. It adopts a robust solution to record and retrieve type information, avoiding information loss and enhancing accuracy. We evaluate DEEPTYPE on Linux kernel, 5 web servers, and 14 user applications. Compared to TypeDive, the prototype of MLTA, DEEPTYPE is able to narrow down the scope of indirect call targets by 43.11% on average across most benchmarks and reduce runtime overhead by 5.45% to 72.95%, which demonstrates the effectiveness, efficiency and applicability of SMLTA.

## 1 Introduction

Indirect call, used commonly to determine the functions to be called at runtime, is a fundamental feature of C/C++ for achieving dynamic program characteristics. Production software (e.g., nginx) and operating systems (e.g., Linux) intensively utilize indirect calls to dynamically adapt program behaviors according to runtime environments and demands, through loading and linking the desired shared libraries.

Precise identification of indirect call targets is of paramount importance, as the control-flow transitions between indirect calls and their respective targets play an essential role in the construction of a global control-flow graph (CFG), which is

extensively adopted in various security-related fields. Static analysis tools rely on CFG for bug detection and program hardening [17, 20, 22, 25, 43, 61–63, 66, 68], program partitioning and privilege separation [5, 8, 18, 26, 28, 42], pruning redundant paths in symbolic execution [4, 7, 10, 50, 58], and guiding directed fuzzing for specific objectives [3, 9, 32, 36, 38, 39, 47]. Additionally, control-flow Integrity (CFI) defenses [1, 6, 14, 34, 35, 49, 65, 67] have been proposed to mitigate control-flow hijacking attacks. However, the strength of CFI depends on the precision of CFG. Imprecise CFG construction results in advanced attacks that bypass CFI [19, 29, 41, 44, 45, 60].

The key challenge in construction of an accurate CFG is identifying the targets of indirect calls. Modern compilers like GCC and Clang cannot determine these targets without additional analysis and instrumentation. Conservative approaches [65, 67] consider all functions or those with address taken as potential targets for each indirect call, producing a considerable number of false positive edges within CFG, which impair the functionality of the applications built upon CFG and impose unnecessary cost. Data tracking analysis [14, 23, 46, 48, 68] tracks value flow, which pursues accuracy at the cost of high performance overhead while the accuracy depends on the precision of the taint analysis and points-to analysis techniques they employ. Type-based analysis [34, 49, 52] checks function signatures to identify functions whose types match with an indirect call. While this approach is efficient, it is susceptible to false positive targets if many functions share the same type as the actual target.

Multi-layer type analysis (MLTA) [27] was proposed for the purpose of improving the accuracy of type-based analysis. Given the fact that function pointers can be members of composite data structures, the type of a function pointer along with the composite types holding it compose a multi-layer type. For example, if function pointer `ptr` with type `void (int)*` is a member of object `a` with type `struct.A`, the variable `a.ptr` has multi-layer type `void (int)* | struct.A`. A function `f` also has this multi-layer type if it is assigned to `a.ptr`. MLTA matches multi-layer types of functions and indirect calls to refine indirect call targets.

However, multi-layer types introduce challenges in type matching because address-taken functions may be propagated between different multi-layer types through information flow, making it hard to collect all targets for an indirect call (see §2.2). MLTA bypasses the challenges by splitting a multi-layer type into several two-layer types, and adopts each layer’s type as the basic unit for information storage and type matching (see §2.4), which avoids missing targets while producing false positive targets. It relinquishes the type information between spitted layers and weakens the restrictions provided by multi-layer types, thereby negatively affecting accuracy.

This paper proposes an advanced approach, Strong Multi-Layer Type Analysis (SMLTA), to mitigate the false positive targets produced by MLTA. It adheres to the strong restriction that identifies only those functions as targets whose entire multi-layer types match with the indirect calls. SMLTA addresses the challenges in multi-layer type matching by resolving the relationships between multi-layer types based on the directions of information flow, and utilizes an adapted breadth-first search (BFS) algorithm [56] to discover all multi-layer types engaged in the propagation of target functions. It also employs a conservative strategy to deal with ambiguous type information due to information flow.

We implemented SMLTA within a prototype, DEEPTYPE,<sup>1</sup> which contains two working phases: 1) information collection and 2) target identification. In the first phase, DEEPTYPE establishes and maintains the mappings between multi-layer types and their associated functions (§4.1). The collected multi-layer types are organized in a hierarchical manner for the purpose of quick retrieval (§4.2). It also preserves the relationships between multi-layer types as indicated by the directions of information flow, facilitating the tracing of multi-layer types engaged in function propagation (§4.3). In the second phase, DEEPTYPE determines the multi-layer type of each indirect call and discovers all other multi-layer types engaged in target propagation (§5.1). Then, it verifies whether the engaged multi-layer types match with the indirect call to precisely identify associated functions as targets (§5.2). Additionally, DEEPTYPE handles diverse instructions and code patterns in real-world programs to reduce the inaccuracy caused by corner cases.

We evaluated DEEPTYPE on Linux kernel, 5 server programs, and 14 user-level applications. We compared it with TypeDive (i.e., the prototype of MLTA), as MLTA is the-state-of-the-art approach in type-based analysis. The results indicate that DEEPTYPE outperforms TypeDive in the precision of indirect call target identification, reducing the average number of indirect call targets by 43.11% on average across most benchmarks. In terms of performance, DEEPTYPE decreases the runtime overhead by 5.45% to 72.95% and achieves lower memory consumption in all evaluated benchmarks. Additionally, a case study on a real-world CVE shows that SMLTA

is more powerful than MLTA in reducing attack surface and preventing exploits.

In summary, this paper makes the following contributions.

- Propose a novel approach called strong multi-layer type analysis (SMLTA) that employs strong restrictions provided by multi-layer types to refine indirect call targets.
- Develop a prototype, DEEPTYPE, which overcomes challenges in multi-layer type matching and utilizes SMLTA to precisely and efficiently identify indirect call targets.
- Evaluate DEEPTYPE with 20 benchmarks and compare it with TypeDive, exhibiting its capability in further refining indirect call targets and reducing both runtime overhead and memory consumption. Additionally, we demonstrate that SMLTA offers a higher level of security.

## 2 Motivation

This section clarifies the challenges in indirect call target identification using multi-layer types, describes how MLTA and SMLTA address these challenges, and highlights the accuracy improvement achieved by SMLTA through an example.

### 2.1 Motivating Example

Listing 1 shows a code snippet with buffer overflow vulnerability. The `strcpy` at line 25 can overwrite the memory location adjacent to `buf` if the length of `msg` is larger than `MAX_LEN`. The adjacent memory location belongs to `w_op`, which is afterwards assigned to `u->uw` at line 26. So, the function pointer `u->uw->low_priv` can point to an address manipulated by the attacker after buffer overflow occurs. At line 29, this function pointer is used to make an indirect call, resulting in arbitrary execution if a lenient CFG is deployed on this program. To prevent such control-flow hijacking attack and other unexpected bugs caused by imprecise CFG, precisely identifying indirect call targets is crucially required.

### 2.2 Challenges

The use of multi-layer types presents challenges in matching indirect calls with all potential targets, particularly when functions are propagated across multi-layer types due to information flow. We categorize the challenges into three classes consistent to three forms of information flow.

First, type assignment and casting operations can transform one multi-layer type into another, resulting in information flow from the original to the transformed type, as well as affecting members of composite types. For example, the type assignment operation (line 26) indicates information flow from `w_op` to `u->uw`, as well as `w_op->low_priv` to `u->uw->low_priv`. In this context, the function `write_to_shared_mem` with multi-layer type `void (char*)* | struct.Write` (line 7), should be propagated to `void (char*)* | struct.Write | struct.User`. Because information flow affects

<sup>1</sup>DEEPTYPE is available at <https://github.com/s3team/DeepType.git>.

```

1 typedef void (*fp)(char*);
2 struct Write {fp low_priv; fp high_priv;};
3 struct User {struct Write *uw; ...};
4 struct Kernel {struct Write *kw; ...};
5
6 void func_init(struct Write *w_op, struct Kernel *k) {
7     w_op->low_priv = &write_to_shared_mem;
8     w_op->high_priv = &write_to_protected_mem;
9     k->kw->low_priv = &write_to_protected_mem;
10    k->kw->high_priv = &write_to_kernel_mem;
11 }
12
13 void user_priv_write(fp icall_ptr, char *buf) {
14     ...
15     (*icall_ptr)(buf);
16 }
17
18 void write_to_mem (char *msg) {
19     struct Kernel *k;
20     struct User *u;
21     struct Write *w_op;
22     char buf[MAX_LEN];
23     func_init(w_op, k);
24     strcpy(buf, msg); // buffer overflow
25     u->uw = w_op;
26     ...
27     if (user_mode()) {
28         if (low_priv()) (*u->uw->low_priv)(buf);
29         else user_priv_write(u->uw->high_priv, buf);
30     }
31 }

```

**Listing 1: A program vulnerable to control-flow hijacking attack through indirect call.** The strcpy at line 25 has buffer overflow vulnerability, which allows attackers to rewrite the function pointer `u->uw->low_priv` and redirect control-flow through the indirect call at line 29.

individual layers as well as overall multi-layer types, it is challenging to track various multi-layer types involved in function propagation and identify all potential targets.

Second, a function pointer performing as an actual parameter can sometimes discard outer layers during parameter passing, leading to discrepancies of type information at different positions. For instance, the actual parameter `u->uw->high_priv` (line 30) has multi-layer types `void (char*)* | struct.Write` and `void (char*)* | struct.Write | struct.User`, while the corresponding formal parameter `icall_ptr` (line 13) has type `void (char*)*`. The obscured outer layers can result in mismatch of multi-layer types, making it challenging to identify all potential targets for an indirect call that uses a formal parameter.

Third, some mechanisms, such as virtual tables [57] used by compilers, can introduce information flow between composite types (e.g., `struct.Write`) and general pointer types (e.g., `char*`). These general pointer types can hinder function propagation since they do not have associated functions, resulting in missing potential targets.

### 2.3 Traditional Type-Based Analysis

Traditional type-based analysis examines the signatures of address-taken functions and the types of indirect calls. If these types match, the function is identified as a potential target. This approach is not impacted by the challenges described in Section 2.2 because it solely relies on the types of function pointers, ignoring composite data structures holding them.

Type	Index	Functions
<code>void (char*)*</code>	-	<code>write_to_shared_mem(7)</code> <code>write_to_protected_mem(8,9)</code> <code>write_to_kernel_mem(10)</code>
<code>struct.Write</code>	0	<code>write_to_shared_mem(7)</code> <code>write_to_protected_mem(9)</code>
	1	<code>write_to_protected_mem(8)</code> <code>write_to_kernel_mem(10)</code>
<code>struct.User</code>	0	-
	...	-
<code>struct.Kernel</code>	0	<code>write_to_protected_mem (9)</code> <code>write_to_kernel_mem(10)</code>
	...	-

**Table 1: Mappings between types and functions in MLTA for Listing 1.** MLTA splits multi-layer types into two-layer types and maintains mappings between these types and associated functions. The two-layer types are represented by a composite type along with an index, which indicates the member type at a specific position. For example, `struct.Write` with index 0 represents the two-layer type `void (char*)* | struct.Write`. The numbers in parenthesis indicate the line numbers where the functions are confined to the types.

In Listing 1, the indirect call at line 29 has type `void (char*)*`, which matches with functions `*shared*`,<sup>2</sup> `*protected*`, and `*kernel*`. As a result, all of them are identified as targets though only `*shared*` is the real target. Similarly, the indirect call at line 15 also has the three targets while only function `*protected*` is the real target.

### 2.4 MLTA

MLTA utilizes the extra type information extracted from composite data structures and supports field-sensitivity considering that a composite data structure may have multiple members holding different functions. If one function is assigned to a pointer, MLTA records the mappings between the multi-layer type and the function, which is called "type-func confinement". It splits multi-layer types and uses each layer type along with an index as key, as Table 1 shows. Similarly, the original and transformed types in type assignment and casting operations are logged in a split manner as well.

In Listing 1, the indirect call at line 29 has multi-layer type `void (char*)* | struct.Write | struct.User`. MLTA identifies potential targets by collecting associated functions for each layer and calculating the intersection to find common functions. For the first layer `void (char*)*` and the second layer `struct.Write` with index 0, both have no original type. Thus, MLTA retrieves the associated functions from Table 1, resulting in set `{*shared*, *protected*, *kernel*}` for the first layer and set `{*shared*, *protected*}` for the second layer. The third layer `struct.User` with index 0 has an original type `struct.Write` (line 26), thus MLTA gathers the associated functions for both types, generating a set `{*shared*`,

<sup>2</sup>In example descriptions, we use simplified function names for readability. For instance, we use `*A*` to represent `write_to_A_mem`.

Type	Functions
<code>void (char*)*   s.Write#0</code>	<code>write_to_shared_mem(7)</code>
<code>void (char*)*   s.Write#1</code>	<code>write_to_protected_mem(8)</code>
<code>void (char*)*   s.Write#0   s.Kernel#0</code>	<code>write_to_protected_mem(9)</code>
<code>void (char*)*   s.Write#1   s.Kernel#0</code>	<code>write_to_kernel_mem(10)</code>

**Table 2: Mappings between types and functions in SMLTA for Listing 1 program.** SMLTA treats each multi-layer type as a whole and uses the entire multi-layer type as a basic unit in storage-purposed data structures. In this table, the structs are abbreviated as "s". The index of each member in a composite type is denoted as "#N" where N is a number. For instance, `s.Write#0` represents `struct.Write` with index 0.

`*protected*`, `*kernel*`}. Finally, it computes the intersection of these three sets. The common functions in resulting set `{*shared*`, `*protected*`} are identified as targets. The indirect call at line 15 with type `void (char*)*` has no original type. So, MLTA directly generates the target set `{*shared*`, `*protected*`, `*kernel*`}, according to Table 1. In contrast with tradition type-based analysis, MLTA narrows down the target set for the indirect call at line 29, but there is still a visible gap between MLTA result and ground truth.

In MLTA, the first challenge is addressed by splitting multi-layer types. The complex information flow between them is simplified to straightforward flow between individual types, which is easier to track. The second challenge is addressed by conservatively confining a function to each layer of its multi-layer type, ensuring no missing target even if the outer layers are discarded. To overcome the third challenge, MLTA marks all general pointer types and composite types that interact with them as "escaping types". It skips the layers with escaping types when calculating intersection, which removes the impact of general pointer types.

## 2.5 SMLTA

SMLTA employs entire multi-layer types as keys for information storage, as Table 2 shows, to circumvent the false positive targets caused by splitting multi-layer types. The relationships between multi-layer types are recorded in the same way. We call multi-layer type  $T_2$  a "friend type" relative to multi-layer type  $T_1$  if information flows from  $T_2$  to  $T_1$  (i.e., a function may be propagated from  $T_2$  to  $T_1$ ). To identify targets for an indirect call, SMLTA exhaustively searches for its friend types and gathers all associated functions as targets.

In Listing 1, the indirect call at line 29 has multi-layer type `void (char*)* | struct.Write#0 | struct.User#0` where "#0" indicates the index. SMLTA exhaustively discovers all friend types that may have information flowing to this multi-layer type, only `void (char*)* | struct.Write#0` in this example, and then gathers associated functions of these multi-layer types. The resulting set `{*shared*`} contains the identified target, which is exactly the real target. The indirect call at line 15 has type `void (char*)*`. Because the function pointer `icall_ptr` is a parameter, SMLTA adds a "fuzzy type" as its

outer layer, which matches with any type. Thus, this indirect call can match with all address-taken functions whose first layer is `void (char*)*`, resulting in the target set `{*shared*`, `*protected*`, `*kernel*`} without missing potential targets.

In SMLTA, the first challenge is addressed by maintaining the relationships between multi-layer types and the exhaustive search of all friend types engaged in function propagation. The second challenge is addressed by fuzzy type, which conservatively admits that all types could possibly match with the discarded outer layer types, ensuring no missing targets. The third challenge is also solved by conducting an exhaustive search of friend types. This search treats general pointer types as bridges between composite types, unblocking function propagation stuck on general pointer types.

## 3 Overview

The prototype of SMLTA is called DEEPTYPE, which contains two phases, as is shown in Figure 1.

Given bytecode file(s) as input, phase 1 analyzes initialization instructions and type propagation instructions to collect information. An initialization instruction assigns a function to a function pointer. We say, it "confines" the function to the corresponding multi-layer type. The mappings between the entire multi-layer types and associated functions are stored in *Type-Func Map*. For quick access and retrieval purpose, DEEPTYPE archives these multi-layer types in *Type Lookup Maps* in a hierarchical manner using multi-layer mappings. Type propagation instructions include type assignment and casting instructions that possibly propagate functions from one multi-layer type to another through information flow. DEEPTYPE records the mappings between destination and source multi-layer types of information flow in *Type-Type Map* using entire multi-layer types as keys and values. The sources are "friend types" relative to destinations.

In phase 2, DEEPTYPE analyzes each indirect call instruction to figure out its multi-layer type. If the function pointer is a formal parameter, fuzzy type is added to represent potentially discarded outer layers. Then, DEEPTYPE exhaustively searches for friend types from *Type-Type Map*, retrieves multi-layer types that match with the indirect call or its friend types from *Type Lookup Maps*, and obtains associated functions from *Type-Func Map*. The union of all associated functions are potential targets for the indirect call. Finally, DEEPTYPE outputs a list of indirect calls in the analyzed program along with their locations and respective targets.

## 4 Phase 1: Information Collection

This section presents how SMLTA collects information from initialization and type propagation instructions, and how it organizes multi-layer types hierarchically.

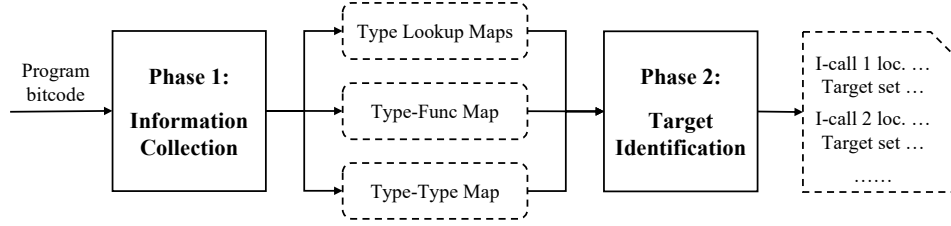


**Figure 1: Workflow of DEEPTYPE.** DEEPTYPE contains two working phases. In phase 1, it collects and records type information in three data structures. In phase 2, it refers to the recorded type information to discover friend types, gather associated functions, and identify targets.

## 4.1 Type-Function Confinements

A function could be considered as a potential target of an indirect call only if it is utilized to initialize local and/or global variables. We confine the function to the multi-layer type of the initialized function pointer by establishing a mapping between them in *Type-Func Map*. It is straightforward to determine the multi-layer types of local variables, by extracting the types layer by layer as they are loaded. However, the multi-layer types of formal parameters and nested global variables may not be fully ascertainable using the same method.

The multi-layer type of a formal parameter is uncertain because it may have extra outer layers that are lost during parameter passing. To complete its multi-layer, we introduce *fuzzy type*, as defined in Definition 1, to cover for missing layers. The fuzzy type can be matched with any type. For instance,  $void(int)^* \mid \text{fuzzy type}$  matches with any multi-layer type whose first layer is  $void(int)^*$ , including  $void(int)^*$ ,  $void(int)^* \mid struct.A\#0$ , and  $void(int)^* \mid struct.A\#0 \mid struct.X\#0$ , etc. Similarly, when an index is uncertain,<sup>3</sup> we employ *fuzzy index* to conservatively match with any index.

**Definition 1** *Fuzzy type marks the type of an uncertain layer. The existence of this layer is uncertain, and the type of this layer is uncertain. In type verification, a fuzzy type can match with any type, even if the corresponding layer does not exist.*

A nested global variable is one that initializes members of other variables, thus may have extra layers involved in other initialization instructions. Its multi-layer type is uncertain when analyzing the instruction initializing it. To gather complete type information, we track all variables that hold this global variable iteratively. For instance, Listing 2 shows a nested global variable `x86_64_elf32_vec` (line 8) with type  $struct.bfd\_target$ , which initializes a member of another global variable `_bfd_target_vector` (line 13). Thus, the function pointer `_bfd_read_ar_hdr_fn` (line 4), as a member of the global variable, should be confined to both  $void(bfd^*) \mid struct.bfd\_target\#53$  and  $void(bfd^*) \mid struct.bfd\_target\#53 \mid vector.bfd\_target\#237$ , ensuring that a potential target could be identified through both multi-layer types.

<sup>3</sup>In LLVM IR, index is typically derived from `GetElementPtrInst` when the corresponding operand is a constant. However, index may be non-constant operand such as a `phi` instruction, indicating an uncertain index until runtime.

```

1 typedef struct bfd_target
2 {
3     ...
4     void* (*_bfd_read_ar_hdr_fn) (bfd *);
5     ...
6 } bfd_target;
7
8 extern const bfd_target x86_64_elf32_vec;
9     ...
10 static const bfd_target * const _bfd_target_vector[] =
11 {
12     ...
13     &x86_64_elf32_vec, // nested global variable
14     ...
15 };

```

**Listing 2: Nested global variable.** `x86_64_elf32_vec` is a nested global variable because it serves as a member in another global variable `_bfd_target_vector`. This example is from `targets.c` from `binutils-2.35`.

## 4.2 Multi-layer Type Organization

For efficient access and retrieval, we organize the collected multi-layer types hierarchically using multi-layer mappings and store them in *Type Lookup Maps*. We prepare  $N$  maps for a program, in which the multi-layer types have up to  $N+1$  layers. More details are illustrated in Appendix A.

To archive a multi-layer type  $T$ , the first  $n$  layers of  $T$  is used as a key in the  $n$ -th map (where  $1 \leq n \leq N$ ), and the  $n$ -th layer of  $T$  is stored as the corresponding value. If  $T$  consists of  $M$  layers, where  $M$  is less than  $N$ , only the first  $M$  maps are utilized for storage. Figure 2 shows an outline of *Type Lookup Maps* and exemplifies the utilization of this data structure via two multi-layer types: ①  $void(int)^* \mid struct.A \mid struct.X$  and ②  $void(int)^* \mid struct.B \mid struct.Y \mid struct.P$ .<sup>4</sup>

*The First Map* stores the mapping between the common first-layer type  $void(int)^*$  and respective second-layer types  $struct.A$ , for ①, and  $struct.B$ , for ②. *The Second Map* stores mappings between first-two-layer types and corresponding third-layer types, among which the first entry is for ① and the second entry is for ②. *The Third Map* works in a similar way to store the rest part of ②. If a multi-layer type contains more than four layers, we will establish more maps based the number of layers, to record the rest parts.

<sup>4</sup>The indexes are omitted to simplify the example and emphasize the key point, which is how to hierarchically archive multi-layer types.

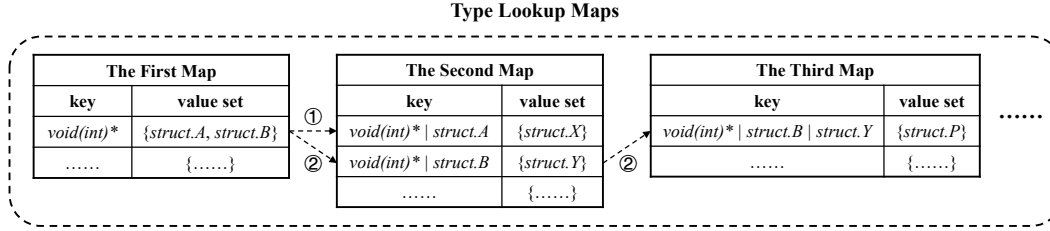


**Figure 2: Outline of Type Lookup Maps with two example types stored.** Type Lookup Maps use multi-layer mappings to archive multi-layer types. The First Map records the first-layer types and corresponding second-layer types; The Second Map records the first-two-layer types and corresponding third-layer types; So on so forth. ①  $void(int)* | struct.A | struct.X$  and ②  $void(int)* | struct.B | struct.Y | struct.P$  are archived as examples.

```

1 struct section_add {...; asection *section;};
2
3 asection *bfd_get_section_by_name (bfd *abfd, const
   char *name);
4
5 copy_object (bfd *ibfd, bfd *obfd, const
   bfd_arch_info_type *input_arch)
6 {
7   ...
8   struct section_add *pupdate;
9   ...
10  pupdate->section = bfd_get_section_by_name (ibfd,
   pupdate->name);
11  ...
12 }

```

**Listing 3: Type assignment.** A variable with multi-layer type *asection* is assigned to another variable with multi-layer type *asection|struct.section\_add#5* in line 10. This example is from objcopy.c in binutils-2.35.

### 4.3 Type Relationship Resolving

A function can be propagated from one multi-layer type to another via type propagation instructions. To collect all involved multi-layer types, we analyze type assignment and casting instructions and introduce *friend type*, as defined in Definition 2, to describe their relationships.

**Definition 2** *A is a friend type relative to B if either of the following holds:*

1. *There exists information flow from A to B.*
2. *There exists information flow from A to C, and C to B.*

*Due to the information flow, the associated functions of A are propagated to B. We say, A "shares" functions with B.*

The second condition manifests that one multi-layer type is a friend type relative to another if there exists a chain of information flow following the first condition. This chain can be as long as the entire program. We record the mapping between one multi-layer type and its *direct friend types*, satisfying the first condition, in *Type-Type Map*. The *indirect friend types*, satisfying the second condition, can be inferred by the recorded relationships.

A type assignment instruction assigns the value of one variable to another. They have different multi-layer types, but share the same first-layer type. Such instructions create a one-way relationship: the source type of information flow is a friend type relative to the destination type. For example, Listing 3 shows a type assignment operation (line 10) where the

```

1 static struct bfd_hash_entry *
2 string_hash_newfunc (struct bfd_hash_entry *entry,
   struct bfd_hash_table *table, const char *string)
3 {
4   struct string_hash_entry *ret = (struct
   string_hash_entry *) entry;
5   ...
6   return (struct bfd_hash_entry *) ret;
7 }

```

**Listing 4: Type casting.** *struct.bfd\_hash\_entry* is casted to *struct.string\_hash\_entry* in line 4. *struct.string\_hash\_entry* is casted to *struct.bfd\_hash\_entry* in line 6. This example is from ecofflink.c in binutils-2.35.

return value of function `bfd_get_section_by_name` is assigned to `pupdate->section`, resulting in information flow from the source type *asection* to the destination type *asection | struct.section\_add#5*, which allows *asection* to share its associated functions with *asection | struct.section\_add#5*.

A type casting instruction transforms one multi-layer type into another, with the first layers of each being distinct. In Listing 4, the original type of `entry` is *struct.bfd\_hash\_entry\** (line 2). It is transformed to *struct.string\_hash\_entry* at line 4. The type casting at line 6 transforms *struct.string\_hash\_entry\** to *struct.bfd\_hash\_entry\**. Considering the flow-insensitivity feature of our static analysis,<sup>5</sup> it is uncertain whether a type casting instruction executes before or after an indirect call, making it uncertain whether the multi-layer type of the indirect call is transformed from another multi-layer type. To address this ambiguity, we conservatively establish a bidirectional relationship between the source and destination types, allowing them to share associated functions with each other so that indirect calls do not miss any potential target.

## 5 Phase 2: Target Identification

This section presents how SMLTA identifies indirect call targets utilizing the type information stored in *Type-Func Map*, *Type-Type Map* and *Type Lookup Maps*.

### 5.1 Friend Type Discovery

For each indirect call, SMLTA examines whether the function pointer is a formal parameter to decide if fuzzy type should be

<sup>5</sup>SMLTA is flow-insensitive for efficiency. Tracking the execution sequence of instructions is beyond our scope.

Before-Part	Fragment	After-Part
	A	lBIC
Al	B	lC
AlBl	C	
	AlB	lC
Al	BlC	
	AlBlC	

**Table 3: A table recording the fragments of multi-layer type AlBlC.** A multi-layer type AlBlC with 3 layers has 6 possible fragments, including single-layer fragments, two-layer fragments, and three-layer fragments.

added to complete its multi-layer type. Once the multi-layer type of an indirect call is ascertained, we discover all of its friend types to ensure that the associated functions shared by the friend types will be identified as potential targets. Given that a multi-layer type can be partially transformed from another type, we extract all possible *fragments*, as defined in Definition 3, to support the exhaustive search of friend types relative to the entire multi-layer type of the indirect call.

**Definition 3** A *fragment* of multi-layer type  $T$  is one or multiple continuous layers in  $T$ .

A multi-layer type with  $N$  layers has  $\frac{(1+N) \times N}{2}$  possible fragments, as exemplified in Table 3. The **Fragment** column lists all possible fragments while the layers before and after each fragment are respectively listed in **Before-Part** and **After-Part** columns. We can substitute each fragment with its friend types and concatenate these types with corresponding Before-Part and After-Part to generate friend types relative to the entire multi-layer type, thereby transforming the task of searching for friend types relative to the multi-layer type into discovering friend types for individual fragments.

For each fragment, the search of direct friend types is straightforward, which is achieved by querying *Type-Type Map*. However, the exhaustive search of indirect friend types can be challenging because these types may be buried in long, cyclic chains of information flow. To address this issue, SMLTA employs an exhaustive search algorithm adapted from Breadth-First Search, which monitors the state of discovered friend types to bypass cycles in chains. This algorithm is detailed in Algorithm 1, where  $\text{Frag}$  represents a fragment and  $\text{Frag}_{ft}$  represents its friend types.

We prepare three sets,  $S_{checked}$ ,  $S_{checking}$ , and  $S_{unchecked}$ , to manage friend types in different states and prevent cyclic search. A friend type currently being used to query the *Type-Type Map* is held in  $S_{checking}$  and is moved to  $S_{checked}$  post-query.  $S_{unchecked}$  holds newly discovered friend types for the next round of search. Initially, the current  $\text{Frag}$  is placed into  $S_{checking}$ . In each search iteration, we look for friend types for elements in  $S_{checking}$  by querying *Type-Type Map* and place newly discovered friend types to  $S_{unchecked}$ . After each iteration, update the three sets for the following round of search. Repeat this process until  $S_{checking}$  is empty and  $S_{checked}$  is no more updated, indicating that all  $\text{Frag}_{ft}$  have been discovered.

---

### Algorithm 1 Exhaustive search of $\text{Frag}_{ft}$

---

**Require:** *Type-Type-Map*,  $\text{Frag}$

**Ensure:** All  $\text{Frag}_{ft}$  are placed in  $S_{checked}$

```

1:  $S_{checked} \leftarrow \{\}$ 
2:  $S_{checking} \leftarrow \{\text{Frag}\}$ 
3:  $S_{unchecked} \leftarrow \{\}$ 
4:  $S_{checked\_origSize} \leftarrow 0$ 
5:  $S_{checked\_newSize} \leftarrow 0$ 
6: while  $S_{checking}$  is not empty do
7:   for  $e$  in  $S_{checking}$  do
8:      $S_{unchecked} = \text{SetMerge}(S_{unchecked}, \text{Type-Type-Map}[e])$ 
9:    $S_{checked\_origSize} = S_{checked}.size()$ 
10:   $S_{checked} = \text{SetMerge}(S_{checked}, S_{checking})$ 
11:   $S_{checked\_newSize} = S_{checked}.size()$ 
12:   $S_{checking}.empty()$ 
13:   $S_{checking} = S_{unchecked}$ 
14:   $S_{unchecked}.empty()$ 
15:  if  $S_{checked\_origSize} == S_{checked\_newSize}$  then return  $S_{checked}$ 

```

---

Given friend types of each fragment, we generate the friend types relative to the entire multi-layer type of an indirect call by concatenation operations, and gather them in a set  $S$  along with the multi-layer type itself for type verification.

## 5.2 Type Verification

The elements in  $S$ , are not exactly the multi-layer types that confine target functions of this indirect call due to three kinds of mismatches: 1) Some friend types generated through fragments do not exist among the recorded multi-layer types; 2) Some elements in  $S$ , containing fuzzy type and index, apparently differ from but actually match with the recorded multi-layer types; 3) Some recorded multi-layer types, containing fuzzy type and index, apparently differ from but actually match with the elements in  $S$ . Hence, we query *Type Lookup Maps* for type verification and collecting *verified types*, which is defined in Definition 4.

**Definition 4** A *verified type* is a multi-layer type that is recorded in *Type-Func Map* and *Type Lookup Maps*, and matches with an element in  $S$ .

To perform type verification, we check each element in  $S$  to find verified types in *Type Lookup Maps*. Given a multi-layer type  $T$  in  $S$ , first of all, we pass the first-layer type of  $T$  to *The First Map* to achieve a scope of second-layer types. Then, check whether the elements in this scope match with the second-layer type of  $T$ . Concatenate the first-layer type with every matched second-layer type to generate a set of first-two-layer types. Lookup *The Second Map* to achieve a scope of third-layer types and find those who match with the third-layer type of  $T$ . Following this working pattern to check the remaining layers until all verified types are retrieved from *Type Lookup Maps*. Finally, query *Type-Func Map* with verified types to find associated functions. The union of such functions are identified as potential targets of the indirect call.

```

store <2 x i64> %12, <2 x i64>* bitcast (i32 ()**
  getelementptr inbounds (%struct.SQLite3Config, %
    struct.SQLite3Config* @sqlite3Config, i64 0, i32
    13, i32 0) to <2 x i64>*), align 8, !dbg !56905, !
    tbaa !11590

```

**Listing 5: A composite instruction.** The store instruction in sqlite is composite, incorporating an embedded bitcast instruction, which in turn is composite and contains an embedded getelementptr instruction.

## 6 Implementation

DEEPTYPE is built on LLVM 15.0 in 2.8k lines of C++ code. It supports C and C++ programs, providing particular advantages for programs that frequently employ composite data structures. This section delineates the enhancements in accuracy and performance from implementation perspective.

### 6.1 Special Handlings

In addition to the novel approach SMLTA, DEEPTYPE enhances accuracy from implementation aspect by addressing diverse instructions and rare code patterns. We identified four typical corners cases and applied special handlings to each, aiming to mitigate inaccuracy resulting from the imprecise processing of these corner cases.

#### 6.1.1 Composite instructions

A composite instruction encapsulates one or more embedded instructions as operands. When analyzing composite instructions, DEEPTYPE cannot acquire complete type information due to the obscured types within the embedded instructions. Listing 5 demonstrates a composite instruction. It is a store instruction that encapsulates a bitcast as its second operand, which itself is also a composite instruction embedding a getelementptr instruction as its first operand.

To gather complete type information, we employ ordered trees to represent hierarchical structure of composite instructions and their embedded instructions, and conduct a systematic analysis of instructions within ordered trees from the lowest to the highest levels, ensuring that the types hidden in embedded instructions can be utilized to generate complete multi-layer types when analyzing their parent instructions. For example, we construct a three-level tree to represent the instructions in Listing 5. The store instruction occupies the root node in level 0, the bitcast instruction is situated in the second child node at level 1, and the getelementptr instruction resides in the first child node of the bitcast at level 2, as Figure 3 depicts. The getelementptr instruction returns a three-layer type `i32()* | struct.sqlite3_mutex_methods#0 | struct.SQLite3Config#13`, which serves as the source type for the bitcast. So, we record it and the destination type `void(int)* | struct.A` as friend types each other in *Type-Type Map*. This relationship contributes to accuracy, but it could be missed without the special handling to composite instructions.

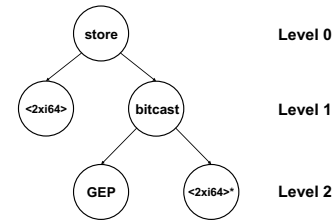


**Figure 3: Ordered tree of the instructions in Listing 5.** The root node represents the composite instruction store. Its child nodes at level 1 denote the instruction’s operands. The second operand is another composite instruction bitcast. The child nodes at level 2 correspond to the operands of bitcast, among which the first one is a getelementptr instruction.

#### 6.1.2 Anonymous structures

In LLVM bitcode, structs are sometimes anonymous when the specific names are not necessary or when they help to optimize the internal representation. This anonymity helps reduce IR size, but can lead to type mismatches, resulting in imprecise target identification.

We address this by assigning a unique identifier to each anonymous struct based on the sequence of member types.<sup>6</sup> This identifier assists in linking anonymous structs to named equivalents elsewhere in the bitcode, thus mitigating inaccuracy caused by mismatches of anonymous structs. If no named equivalent is found, they are named as *struct.anon*, which conservatively matches with any struct, preventing missing targets resulted from anonymous structs.

#### 6.1.3 Dead functions

The iterative updating and patching of applications often results in the presence of dead functions, which are declared but not invoked, thus will not be executed during runtime. The analysis of instructions within these dead functions generates redundant type information, leading to false positive targets and unnecessary performance overhead. To enhance both accuracy and efficiency, our analysis omits dead functions.

#### 6.1.4 Empty Type

In LLVM IR, the notation "{}" is employed to denote an anonymous struct type when the specific details of the data structure are unnecessary and subsequently omitted. We name it as "empty type." Contrary to the anonymous structs discussed in Section 6.1.2, which merely lack names, the empty type is anonymous and contains no fields. However, what it represents can often be inferred from bitcast and other corresponding instructions in proximity. We categorize the code patterns involving empty types into two distinct classes, addressing each class with tailored solutions. Otherwise, the presence of empty type can impact the precision of our analysis as itself does not match with any struct.

<sup>6</sup>As of October 2023, the latest version of TypeDive uses similar method to identify anonymous structs. However, it ignores those anonymous structs whose names never appear in the bitcode, which may lead to missing targets.



When the empty type serves as the destination type in a `bitcast`, we observed that any subsequent utilization of the empty type in IR corresponds to the usage of the source type in source code. Accordingly, we record the source type as a friend type relative to the empty type, mitigating missing targets that may result from type mismatch. Conversely, when the empty type is the source type in a `bitcast`, we observed that its outer layer types in IR are the outer layer types of the destination type in source code. Thus, we record the empty type’s outer layer types as those of the destination type’s, ensuring that complete multi-layer types are gathered for type matching and target identification.

## 6.2 Caches

To diminish the performance overhead, we deploy two caches aiming at reducing runtime cost without affecting accuracy. The first one is used to store the verified types of a multi-layer type so that the exhaustive search algorithm and type verification process only run once for each multi-layer type. The second one is used to store identified targets of an indirect call so that another indirect call with the same multi-layer type can be quickly resolved by accessing the cache.

## 7 Evaluation

We evaluate the effectiveness of DEEPTYPE in Section 7.1 and overhead in Section 7.2, comparing it with TypeDive (commit acb8f4c) since MLTA is the state-of-the-art approach in type-based analysis. Additionally, we evaluate the contribution of SMLTA in accuracy in Section 7.3 and present its security impact through a case study in Section 7.4.

Our evaluation is conducted on linux kernel, 5 web servers and 14 user applications. The GNU Binutils-2.35 is a collection of binary tools. We selected 13 among 15 programs as the discarded ones barely use indirect calls.<sup>7</sup> SQLite-3.45.1 is a database engine which contains numerous multi-layer types. 5 server programs are nginx, httpd, openVPN, proftpd and sshd. We use Linux-5.1 as the benchmark to show the scalability of DEEPTYPE.

Experiments are conducted on Ubuntu 20.04 with 8-core Intel Core i9-9880H CPU @ 2.30GHz and 16GB DDR4 RAM. The benchmarks are compiled by WLLVM [54] with LLVM-15. We use `-g -O0`<sup>8</sup> flags to ensure that the generated bitcode contains debug information and type information, and that the instructions DEEPTYPE analyzes are not optimized out. Another flag `-Xclang -no-opaque-pointers` is used to disable opaque pointers so that pointers’ types are sustained.

<sup>7</sup>The program `sysinfo` does not contain any indirect call; The program `elfedit` only has 53 indirect calls without complex multi-layer types, showing exactly the same result for TypeDive and DEEPTYPE.

<sup>8</sup>This optimization level compiles the fastest and generates the most debuggable IR code, with which we can determine whether a function pointer is a local variable or formal parameter.

To compare with TypeDive, we execute both tools on LLVM-15 and apply dead function elimination on them to make sure the benchmark bitcode analyzed by DEEPTYPE and TypeDive are exactly the same. In the experiments, we deploy 7-layer mappings in *Type Lookup Maps*, which are sufficient to archive the multi-layer types in our benchmarks. Appendix A shows how to determine the number of mappings.

### 7.1 Effectiveness of DEEPTYPE

The effectiveness of DEEPTYPE is demonstrated by its ability to narrow down the scope of indirect call targets. We use Average Number of Targets (ANT) as metric to quantitatively measure effectiveness, which is defined as:

$$ANT = \frac{Num(T)}{Num(IC)},$$

where  $Num(T)$  represents the total number of identified targets,  $Num(IC)$  represents the total number of indirect calls that have targets. While the metric in TypeDive paper [27] is also average number, it only takes into account the indirect calls whose multi-layer types have at least two layers. Their metric neglects the fact that single-layer types can also benefit from MLTA, and that some indirect calls have no target identified because they are not initialized or because DEEPTYPE and TypeDive miss targets due to inevitable obstacles in implementation, as elaborated in Section 8.1. Therefore, we define ANT to precisely evaluate the effectiveness. To clarify *false positive (FP)* and *false negative (FN)* subsequently used in this paper, we define them in Definition 5.

**Definition 5** Given an indirect call, a *false positive (FP)* is a function erroneously included in the target set contrary to the ground truth. A *false negative (FN)* is a function erroneously excluded from the target set contrary to the ground truth.

Table 4 presents the ANT for the benchmarks tested by DEEPTYPE and TypeDive, and the reduction rate in ANT achieved by DEEPTYPE compared to TypeDive. Given that the binutils programs share numerous library functions, leading to analogous ANT value, we only list their average ANT. The details are available in Appendix B. The data in Table 4 indicates that DEEPTYPE reduces the ANT by 43.11% on average across most benchmarks, including binutils, httpd and linux. However, DEEPTYPE does not manage to decrease the ANT for nginx, openvpn and proftpd.

The reduction in ANT can be attributed to SMLTA and special handlings in DEEPTYPE. SMLTA follows the strong restriction that checks the entire multi-layer type of an indirect call to identify targets that match with it. In contrast, TypeDive employs MLTA which separately resolves each layer of a multi-layer type and calculates intersection to determine the target set, potentially leading to FPs. The special handlings in DEEPTYPE are tailored to address corner cases where type

Program	DEEPTYPE	TypeDive	Reduction Rate
binutils	2.47	10.98	77.50%
sqlite	6.24	8.32	25.00%
nginx	6.38	5.60	-13.93%
htpdp	6.23	12.27	49.23%
openvpn	2.35	1.62	-45.06%
proftpd	3.10	2.96	-4.73%
sshd	5.43	5.57	2.51%
linux	9.74	25.17	61.30%

**Table 4: Average number of indirect call targets.** This table shows the average number of indirect call targets, and the reduction rate produced by DEEPTYPE over TypeDive. binutils shows the average of the 13 programs in binutils, the detailed data of each is elaborated in Appendix B.

information may be obscured, which enable DEEPTYPE to extract more accurate type information, thereby reducing FPs.

To validate the reasons for ANT reduction, we conducted a manual analysis on `objcopy`, as it contains substantial yet manageable number of indirect calls. By manually examining the indirect calls for which DEEPTYPE collects fewer targets than TypeDive, we confirmed the contributions of SMLTA and special handlings, and additionally unveiled another factor contributing to the reduction of ANT.

Field-sensitivity deployed in DEEPTYPE enables the differentiation of distinct members within a composite data structure, even if they share the same type, which further refines indirect call targets. Despite the assertion of field-sensitivity in TypeDive paper, our manual analysis discovered FPs due to its field-insensitive. For instance, in a simplified scenario, a function is confined to `i64(i8*)* | struct.bfd_target#13`, whereas an indirect call has multi-layer type `i64(i8*)* | struct.bfd_target#23`, without any type propagation involved. TypeDive identifies this function as a target because its first and second layers respectively match `i64(i8*)*` and `struct.bfd_target`. By contrast, field-sensitive DEEPTYPE mitigates such FPs. Thus, field-sensitivity is another reason for ANT reduction.

Table 4 also shows that DEEPTYPE does not consistently reduce ANT, particularly in the cases of `nginx` and `openvpn`. There are two reasons for the increasing ANT. First, the adoption of fuzzy type leads to the conservative inclusion of all potentially matching types. It decreases FNs meanwhile inevitably brings in FPs, consequently raising the ANT value. Second, the special handlings enable DEEPTYPE to extract more precise type information, diminishing both FPs and FNs. In situations where the reduction in FNs surpasses that in FPs within a program, the ANT value increases. Given that the rising ANT is attributed to the reduction in FNs, it is deduced that DEEPTYPE is theoretically and practically effective in refining indirect call targets.

Figure 4 shows the distribution of indirect calls with different number of targets in linux kernel. We choose linux kernel because it is a complicated program that can demonstrate the distribution patterns as comprehensive as possible. In the experiment, although a number of indirect calls have no target according to either DEEPTYPE or TypeDive or both, we ob-

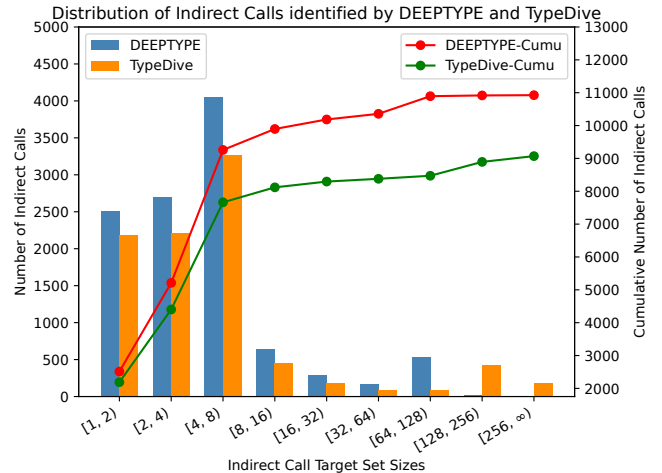


**Figure 4: Distribution of indirect calls with different sizes of target sets in linux.** The y-axis on the left shows number of indirect calls. The y-axis on the right shows cumulative number of indirect calls. The x-axis shows indirect call target sets' sizes ranging from 1 to infinite divided into 9 intervals. DEEPTYPE and TypeDive respectively represents the number of indirect calls reported by DEEPTYPE and TypeDive. DeepType-Cumu and TypeDive-Cumu respectively represents the cumulative number of indirect calls reported by two tools.

serve that DEEPTYPE is capable of finding more valid targets for more indirect calls, thus DEEPTYPE and DeepType-Cumu have more indirect calls than TypeDive and TypeDive-Cumu in most intervals. The main difference between DEEPTYPE and TypeDive falls in intervals [2,4) and [4,8), the number of targets represented by these two intervals is much smaller than the average number of indirect call targets reported by TypeDive. As the number of indirect call targets increases, the difference between DEEPTYPE and TypeDive gradually decreases and becomes trivial except for interval [64,128), where DEEPTYPE has more indirect calls, and interval [128,256), where TypeDive has more indirect calls.

This trend indicates that the ratio of indirect calls with small target sets is lower in DEEPTYPE. We define *small* by different values of threshold in Table 5. A target set is considered as small when its size is less than the threshold. We observe that when the threshold is 2 or 4, DEEPTYPE has lower ratio of indirect calls with small target sets. However, this does not imply that TypeDive outperforms DEEPTYPE for these indirect calls. At lower thresholds (i.e., 2 or 4), a single FP or FN can significantly impact whether an indirect call is categorized as with a small or large target set. Conversely, at higher thresholds, the influence of false reports on categorizing diminishes. Therefore, the general trend is more indicative. In most cases, DEEPTYPE demonstrates a higher ratio of indirect calls with small target sets, underscoring its effectiveness in refining indirect call targets.

Additionally, we compiled the benchmarks on various optimization levels to assess the effectiveness of DEEPTYPE across these levels. The data presented in Table 6 indicates that DEEPTYPE reports higher ANT when the benchmarks

Threshold	DEEPTYPE	TypeDive
2	23.0%	24.1%
4	47.7%	48.5%
8	84.7%	84.5%
16	90.6%	89.5%
32	93.2%	91.5%
64	94.8%	92.4%
128	99.7%	93.4%
256	99.9%	98.1%

**Table 5: Ratio of indirect calls with *small* target sets.** The definition of *small* depends on the threshold. If the indirect call’s target set size is smaller than the threshold value, this indirect call is considered as with *small* target sets. The last two columns respectively show the ratios of indirect calls with *small* target sets in DEEPTYPE and TypeDive.

Program	O0	O1	O2	O3
binutils	2.47	3.20	3.20	3.13
sqlite	6.24	6.46	6.48	6.56
nginx	6.38	8.00	8.02	7.99
httpd	6.23	6.23	6.23	6.23
openvpn	2.35	2.80	2.45	2.45
proftpd	3.10	3.10	3.10	3.10
sshd	5.43	5.43	5.43	5.43
linux	9.74	9.74	9.74	9.74

**Table 6: The effectiveness of DEEPTYPE on different optimization levels.** This table shows the ANT reported by DEEPTYPE when analyzing benchmarks respectively compiled with optimization level O0, O1, O2 and O3.

are compiled with more aggressive optimization settings for the majority of the programs examined. The increasing ANT can be attributed to the fact that higher optimization levels tend to optimize away certain instructions that DEEPTYPE relies upon for analysis, leading to incomplete type information being gathered. Consequently, DEEPTYPE produces an increased number of FPs and FNs. When there is a predominance of FPs over FNs, the ANT increases.

The stability of ANT values across different optimization levels for programs such as http, proftpd, sshd, and linux can be explained by two factors. First, the FPs and FNs caused by the optimized-out instructions achieve a balance, neutralizing the impact on ANT. Second, the minimal number of FPs and FNs does not significantly alter the ANT metric.

Despite the reduced efficacy of DEEPTYPE on higher optimization levels compared to the O0 level, it nevertheless outperforms TypeDive in those benchmarks where DEEPTYPE with O0 optimization surpasses TypeDive. This observation demonstrates that while there is a marginal decrease in effectiveness with higher optimization levels, DEEPTYPE retains its comparative advantage over TypeDive.

## 7.2 Performance

DEEPTYPE employs caches to obviate redundant analysis and improve performance. To evaluate the runtime overhead comprehensively, we disabled the caches in DEEPTYPE, resulting in a variant denoted as DT-nocache. We executed DEEPTYPE, DT-nocache, and TypeDive on each benchmark for three times

to obtain average execution time, which yields more reliable statistics as it helps mitigate the impact of hardware conditions and operating system states through averaging.

Figure 5 presents the execution time for each benchmark. DEEPTYPE significantly outperforms TypeDive, showing a reduction in overhead ranging from 5.45% to 72.95%, with an average reduction of 37.02%. DT-nocache also demonstrates reduced overhead compared to TypeDive, despite TypeDive is equipped with caches.

To deduce the primary source of runtime overhead and reveal the reason for DEEPTYPE’s efficiency, we separately measured the execution time of information collection and target identification phases, considering the shared general workflow of all tools. The experiments were conducted on linux benchmark, which manifests noticeable differences among three tools. According to Figure 6, the percentages of runtime overhead incurred during target identification exhibit a progressive increase among DEEPTYPE, DT-nocache, and TypeDive, standing at 20.6%, 44.2%, and 65.0%, respectively. Thus, the lower overhead of DEEPTYPE should owe to the target identification phase, wherein DEEPTYPE straightforwardly deals with the entire multi-layer type of each indirect call. In contrast, TypeDive addresses each two-layer type within the multi-layer type and calculates intersections, incurring additional runtime overhead. The fact that DEEPTYPE refines indirect call targets also indicates that TypeDive consumes extra computational resources on FPs.

An additional observation reveals that the distinction in runtime overhead is evident in binutils, sqlite and linux, whereas it is negligible in the five server programs. The reason for this distinction is the higher prevalence of multi-layer types with more layers in binutils, sqlite and linux as illustrated in Figure 7. The efficiency advantage of DEEPTYPE over TypeDive is primarily attributed to DEEPTYPE’s one-time resolution on the entire multi-layer type, in contrast to the laborious resolution in TypeDive for each two-layer type. It is noteworthy that a multi-layer type may consist of multiple two-layer types. Consequently, the benchmarks containing a greater number of multi-layer types with more layers amplify the runtime overhead discrepancy between DEEPTYPE and TypeDive.

Typically, memory overhead is not a main concern in static analysis, as tools that offer efficient performance without compromising precision are often favored. We still measure the memory overhead of DEEPTYPE using Massif tool in Valgrind [31] tool suite with `-pages-as-heap=yes` option enabled, to measure all the memory used, and compare it with TypeDive for a thorough performance assessment.

Figure 8 shows the memory overhead of DEEPTYPE and TypeDive. Regarding user applications and server programs in the benchmarks, both tools exhibit memory overhead below 150 MB. However, in the context of the Linux kernel, both DEEPTYPE and TypeDive demonstrate higher memory overheads ranging from 4.2 GB to 4.3 GB. This discrepancy is attributed to the larger size of kernel program, which involves

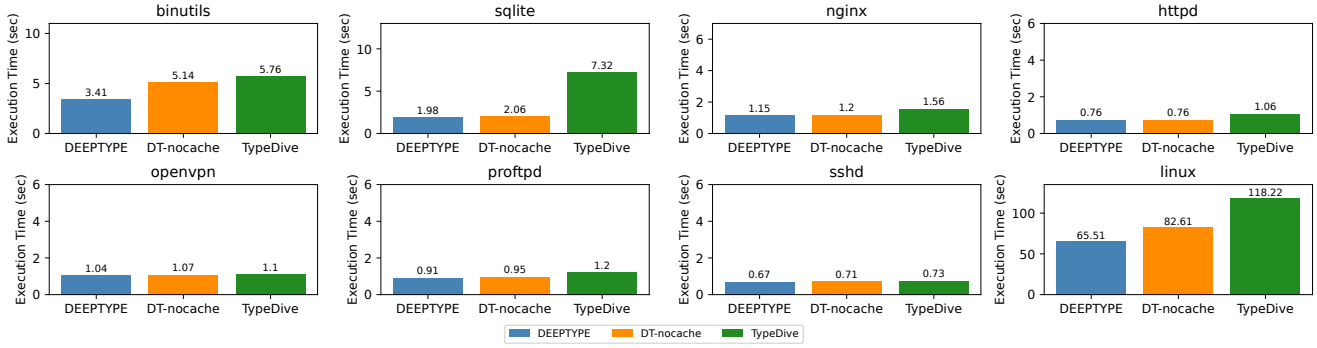


**Figure 5: Execution time of DEEPTYPE, DT-nocache and TypeDive.** DT-nocache represents DEEPTYPE without caches deployed. For each benchmark, we plot a bar chart to depict the execution times of DEEPTYPE, DT-nocache, and TypeDive, and the y-axis scale of which is adjusted to encompass the full data range without excessive magnification, allowing for clear differentiation in execution times. Specifically, the binutils chart illustrates the average execution times across all assessed binutils programs.

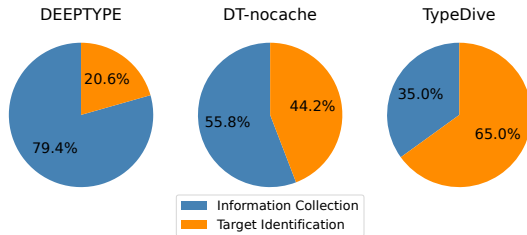


**Figure 6: Runtime overhead distribution of DEEPTYPE, DT-nocache and TypeDive.** DEEPTYPE and TypeDive follow the same general workflow that contains two phases: 1) collect information and record it in data structures, 2) analyze indirect call sites and recorded information to identify targets.

more multi-layer types. As a result, both tools record a greater volume of type information, leading to increased sizes of data structures and consequently consuming more memory spaces.

DEEPTYPE shows lower memory overhead than TypeDive, while the subtle difference between two tools remains consistent across all benchmarks. This consistency is attributed to the comparable memory space occupied by the data structures in two tools. Although DEEPTYPE records entire multi-layer types, which have larger sizes than two-layer types, it allocates fewer entries in maps for storage. The difference is due to the additional memory space utilized in TypeDive for recording escaping types, which is designed to overcome the third challenge, as elaborated in Section 2. In contrast, DEEPTYPE adopts the exhaustive search algorithm which does not consume so much memory space as escaping types.

### 7.3 Contribution of SMLTA in Accuracy

As described in Section 7.1, DEEPTYPE is capable to narrow down the scope of indirect call targets. This capability owes to SMLTA and special handlings to corner cases. To further investigate the impact of SMLTA on effectiveness, we disabled the special handlings in DEEPTYPE, resulting in a variant denoted as DT-noSH. Different ANT values of DEEPTYPE and DT-noSH exhibit the impact of special handlings, thus

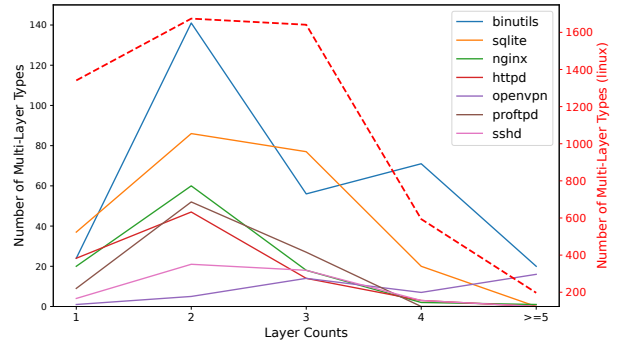


**Figure 7: Number of multi-layer types with different layer counts.** The y-axis on the right shows the number of multi-layer types in linux while the y-axis on the left shows the number of multi-layer types in other benchmarks.

revealing the contribution of SMLTA.

Table 7 presents the ANT reported by DEEPTYPE and DT-noSH. The ANT of DT-noSH is close to that of DEEPTYPE, indicating that disabling the special handlings has minimal impact on the effectiveness of DEEPTYPE, which reveals the primary role of SMLTA in accuracy improvement. The rationale behind the statistics is that the special handlings are specifically implemented to address corner cases. Without them, DEEPTYPE generates slightly more FPs and FNs. Given the definition of ANT, minor fluctuations in the total number of indirect call targets do not significantly alter ANT value when the volume of indirect calls is relatively high. Nonetheless, these special handlings remain crucial, as they play a vital role in mitigating the FPs and FNs that are orthogonal to SMLTA.

Recall that there are four special handlings. First, the systematic analysis of composite instructions facilitates the generation of complete multi-layer types. Among all the benchmarks, nginx and linux exhibit the most significant improvement owing to this special handling, given their relatively higher prevalence of composite instructions. Second, linking anonymous structs with named equivalents enables DEEPTYPE to accurately recognize and match multi-layer types. We observe that openssl and linux obtain the most ben-

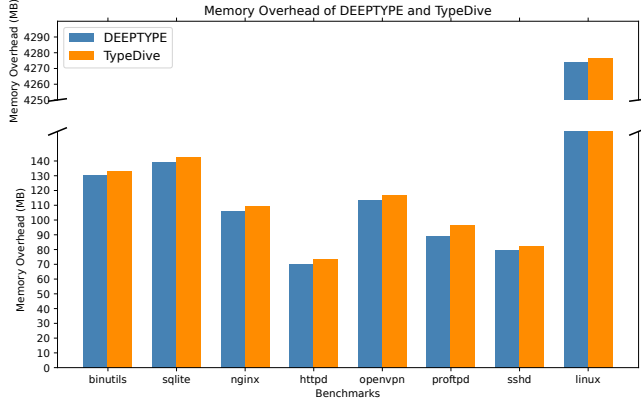


**Figure 8: Memory overhead of DEEPTYPE and TypeDive.** The scales from 150 to 4250 on y-axis are cut out because there is a gap between the memory overheads of linux and other benchmarks. DEEPTYPE always has lower memory overhead than TypeDive while the difference between two tools is consistently subtle.

Program	DEEPTYPE	DT-noSH	DT-weak
binutils	2.47	2.48	2.70
sqlite	6.24	6.33	6.97
nginx	6.38	8.62	12.99
httpd	6.23	6.23	7.66
openvpn	2.35	2.39	2.35
proftpd	3.10	3.13	4.22
sshd	5.43	5.42	5.43
linux	9.74	9.72	13.09

**Table 7: ANT values of DEEPTYPE, DT-noSH and DT-weak.** DT-noSH exhibits the contribution of SMLTA. DT-weak shows the impact of storing entire multi-layer types in *Type-Func Map*.

efit from this special handling compared to other benchmarks. Third, DEEPTYPE eliminates dead functions to discard redundant information, thereby mitigating FPs. All benchmarks, except for httpd and openvpn, benefit from this special handling. Last, DEEPTYPE handles empty types accordance to specific code patterns. Due to the infrequent occurrence of the empty type, its impact on ANT is negligible.

Although the comparison between DEEPTYPE and DT-noSH reveals the significant contribution of SMLTA to effectiveness, we also implemented a weak version of DEEPTYPE, denoted as DT-weak, which stores two-layer types in *Type-Func Map*, to help examine the impact of recording entire multi-layer types. As depicted in Table 7, DT-weak demonstrates a higher ANT than DEEPTYPE across most benchmarks, indicating that recording entire multi-layer types, rather than two-layer types, effectively refines indirect call targets. The difference between two tools is particularly evident on nginx and linux, which contain relatively more complex multi-layer types than other benchmarks. Note that, DT-weak still benefits from SMLTA because only the method of recording multi-layer types in *Type-Func Map* has been modified, while other SMLTA designs, such as multi-layer mappings, continue to play a role in filtering out FPs.

```

1 void track_set_index (...) {
2     ...
3     track->index[i] = ind;
4 }
5
6 static gboolean get_file_metadata (...) {
7     TrackerExtractInfo *info;
8     ...
9     tracker_extract_info_unref(info);
10    ...
11 }
12
13 gboolean g_option_context_parse (...) {
14     ...
15     if (!(* group->pre_parse_func) (context, group,
16                                     group->user_data, error))
17 }

```

**Listing 6: CVE-2023-43642 vulnerable code.** Line 3 is vulnerable to out-of-bounds access. An exploit for this vulnerability can overwrite a function pointer in glib to gain code execution.

## 7.4 Case Study

While SMLTA is a fundamental tool applicable across various security-related fields (e.g., static bug detection, symbolic execution, fuzzing, and etc.), we demonstrate its security impact through the example of CFI enforcement.

CVE-2023-43641 [11] is an out-of-bounds access that enables arbitrary write in libcue. As detailed in Listing 6 at line 3, both the value of index *i* and *ind* can be controlled by attacker. By setting the index *i* negative, an attacker can achieve arbitrary write through preparing the value of *ind*. The exploit [2] utilized this vulnerability to corrupt a function pointer in glib (cross-referenced by libcue) to achieve arbitrary code execution. To be specific, the exploit overwrites the heap object *info* (line 7), which is allocated in a function invoked by *track\_set\_index* (line 1). This overwrite enables the corruption of function pointer *pre\_parse\_func* (line 15) in glib, and the corrupted function pointer is subsequently used to call the *initable\_init* function, which behaves similarly to the *system* function, enabling arbitrary code execution.

Similar to many typical CVE exploits, this exploit assumes Control Flow Integrity (CFI) is not deployed. The function pointer *pre\_parse\_func* has a type mismatch with the target function *initable\_init*, making the exploit preventable by both MLTA and SMLTA. However, this does not imply that the vulnerability can be completely mitigated by either MLTA or SMLTA, as attackers may still conduct exploits by corrupting alternative function pointers.

We further examined glib and revealed 5 function pointers that can bypass MLTA, see Table 8. MLTA fails to prevent the exploits that corrupting these function pointers because it identifies the function *initable\_init* as a valid target for these function pointers, though it is a FP in fact. This FP can be attributed to MLTA’s approach of splitting multi-layer types, which confines the function *initable\_init* respectively to *gboolean* (*Ginitable\**, *Gancellable\**, *GError\*\**)\*

Function Pointers	MLTA	SMLTA
callback	✗	✓
callback*	✗	✓
traverse_func	✗	✓
func	✗	✓
predicate	✗	✓

**Table 8: The capability of MLTA and SMLTA in preventing exploits.** The listed function pointers, located in `glib`, can be corrupted through the vulnerability. MLTA fails to prevent the exploits through the 5 function pointers while SMLTA can prevent these exploits. To differentiate two function pointers named "callback" in separate functions, one is denoted as "callback\*".

and `struct._Ginitableface` with index 1, weakening the restriction of multi-layer type matching.

For example, `traverse_func` in Table 8 has type `gboolean (gpointer*, gpointer*, gpointer*)*`, which matches with `gboolean (Ginitable*, Gancellable*, GError**)*` due to information flow in `glib`. Thus, MLTA identifies `initable_init` as a potential target, enabling attackers to rewrite the function pointer with the address of `initable_init` and achieving arbitrary code execution.

In contrary, SMLTA is able to prevent these exploits because it strictly confines `initable_init` to its entire multi-layer type `gboolean (Ginitable*, Gancellable*, GError**)* | struct._Ginitableface#1`, which does not match with any function pointer in Table 8. Consequently, SMLTA effectively reduces the attack surface of control-flow hijacking attacks utilizing this vulnerability. By limiting the attacker’s ability to corrupt function pointers, SMLTA offers a higher level of security compared to MLTA in CFI implementation.

## 8 Discussion

### 8.1 Soundness

This section discusses the soundness of SMLTA. In theory, SMLTA belongs to type-based analysis, the soundness of which has already been proved [30, 33, 37, 53, 59]. In general, the static analysis in DEEPTYPE is flow-insensitive, indicating that it does not track the sequences of instructions or data-flow between basic blocks, but purely collects type information, which does not yield any FN.

Specifically, SMLTA contains 4 novel designs, none of which produces FNs. First, fuzzy type and fuzzy index stand for uncertain layers and indexes. They match with any type and index to ensure that no potential targets can be missed. Second, multi-layer mappings are used to archive the collected multi-layer types without any omission. It does not produce any FN because all recorded multi-layer types can be retrieved through querying the mappings. Third, the relationships among multi-layer types involved in an information flow chain is conservatively recorded. Any potential information flow between two multi-layer types is considered when identifying targets. Finally, the exhaustive search algorithm discovers all friend types that can share associated functions

with the multi-layer type of the indirect call, ensuring all potential targets being identified.

### 8.2 Limitations

The implementation of DEEPTYPE does not robustly address all corner cases in real-world programs. Besides the ones addressed in Section 6, some corner cases are out of our scope. For example, LLVM IR only contains type information but omits instantiated values of the members in global variables with composite type. If a function pointer as a member of a global variable is initialized at the global scope, the function assigned to it is apparent in source code but does not appear in the corresponding IR, thus does not appear in bitcode.<sup>9</sup> Given this fact, DEEPTYPE is unable to record the mappings between multi-layer types and functions for such initialization instructions, resulting in missing targets for involved indirect calls. Take `binutils` programs as another example, some indirect call targets are functions in the GNU linker, LD, while we use Clang to compile the programs which uses LLD as linker.

Albeit the accuracy improvement contributed by SMLTA and special handlings, DEEPTYPE still exhibits deficiencies in terms of accuracy. For small programs that contain few complicated multi-layer types, DEEPTYPE is limited in reducing FPs compared to TypeDive meanwhile possibly yielding extra FPs instead due to the conservative design and implementation choices for soundness purpose. In addition, if several function pointers have the same multi-layer type but points to different functions, SMLTA produces FPs in this scenario.

In evaluation aspect, there is no standard scale available to calculate the statistics such as FP rate, FN rate and accuracy, due to the absence of ground truth. Although “pseudo ground truth” [24] is a feasible solution, it highly depends on the precision of dynamic analysis adopted. If the dynamic analysis result is not proved to be extremely close to the ground truth, the numerical data of soundness and precision relative to the pseudo ground truth is not convincing subsequently. We use ANT as metric to reflect the accuracy improvement. But it is convincing only in the context that both SMLTA and MLTA pertain to type-based analysis and the novel designs in DEEPTYPE does not produce FNs.

### 8.3 Future Work

SMLTA generates FPs when multiple functions share the same multi-layer type with an indirect call. This is a limitation intrinsic to type-based analysis that relies solely on type verification. To enhance accuracy, we intend to integrate data-flow analysis with SMLTA, assessing both value and multi-layer type to further constrain potential targets, thereby reducing the FPs inherent to SMLTA. To maintain a balance between accuracy and performance, this data-flow analysis will be designed to be lightweight, focusing on intra-procedural analysis.

<sup>9</sup>Bitcode is a binary encoding of LLVM IR.

Motivated by the absence of a standard and reliable metric for comparing various approaches, we also plan to develop a benchmark that includes a comprehensive ground truth. This ground truth will encompass, but is not limited to, indirect call targets, alias pointers, and value sets. This will enable a wide range of basic tools used in both static and dynamic analysis to evaluate their effectiveness, identify the fundamental reasons for any inaccuracies, and enhance their design and implementation accordingly.

## 9 Related Work

**Conservative solutions.** Zhang et al. propose a protection mechanism called CCFIR [65] which implements a policy pertaining to indirect control transfers. It prohibits any indirect calls/jumps to locations other than those included in a white-list, which is derived from the relocation tables of ASLR [55] that provides absolute addresses of valid functions. Similarly, Zhang and Sekar [67] conservatively count all valid functions as targets given the assumption that source code is not available. These solutions are exceedingly conservative and may produce numerous false positives targets.

**Type-based analysis.** In cases where the source code of a program is available, types of function pointers are utilized to deduce potential targets. Each indirect call is restricted to being directed towards only the functions with the same type. Tice et al. present VTV and IFCC that provide forward-edge CFI protection respectively for GCC and LLVM [49]. VTV conducts a validation process to ensure the correctness of the vtable pointer used for a virtual call by confirming the vtable pointer to be used for the indirect call points either to the vtable for the static type of the object, or to a vtable for one of its descendant classes. IFCC forces a function pointer into the right function-pointer set in jump tables to mitigate CFI violations and each function-pointer set has a specific function type signature. Niu and Tan present MCFI [34] where an indirect call is allowed to call any address-taken function whose type is structurally equivalent to the function pointer's type. Victor et al. propose TypeArmor [52] to reduce the number of targets for indirect calls where function type and argument number is checked to identify valid targets. MLTA [27] utilizes multi-layer type, which includes function type signature and type of composite data structures, to significantly refine indirect call targets. The majority of the prior work on resolving C++ virtual functions depend on class hierarchy analysis combined with object type information [15, 21, 40, 49, 64]. These approaches employ an expanded single-layer type to identify targets, but our approach can further improve the accuracy by utilizing types of multiple involved data structures.

**Data tracking Analysis.** Ge et al. utilize taint analysis in their fine-grained CFI to identify targets for kernel software [14]. They begin with a function and taint all function pointers that are initialized with the function or the tainted function pointers. If a function pointer is in a structure, they taint the

field for all memory objects of that structure's type. This policy enables fine-grained CFI to leverage the information of directly related data structure instead of only considering the function pointer itself, but it is still less precise than SMLTA which uses type information of all involved data structures to restrict targets. Kim et al. use block-based pointer analysis (BPA) [23] to identify indirect call targets, which generates memory blocks for heaps, stack frames, and global data sections following specific rules and perform pointer analysis in each memory block to infer points-to relationships. They also upgrade BPA by offset-sensitivity in BinPointer [24], which tracks the offset in each memory block for more fine-grained pointer analysis. Compared with strong MLTA, such approach is deficient in handling type casting, which will cause missing targets. Another limitation is that it does not support C++. CF-GAccurate [46] interleaves four techniques including forced execution, backward slicing, symbolic execution and value set analysis to construct CFG, which is precise at the expense of high performance overhead.

**Dynamic Analysis.** Many other solutions [12, 13, 16, 35, 51] use dynamic analysis which relies on runtime information to identify indirect call targets. These solutions address a distinct problem area, which is the assurance of the validity of a runtime target. Conversely, our work statically deduces the range of potential targets for each indirect call.

## 10 Conclusion

In this paper, we have introduced strong multi-layer type analysis (SMLTA), a novel approach in refining indirect call targets, that thoroughly utilizes type information provided by multi-layer types. It treats the entire multi-layer type as a basic unit for information storage and type verification to improve accuracy. SMLTA resolves relationships between multi-layer types, exhaustively discovers friend types for indirect calls, and employs fuzzy type to overcome the challenges in indirect call target identification using multi-layer types. Additionally, multi-layer mappings are deployed to hierarchically archive multi-layer types for quick access. We implemented SMLTA in DEEPTYPE, which is equipped with special handlings to address diverse code patterns and corner cases. DEEPTYPE is scalable to large applications with superior effectiveness as well as performance. The experiment results showed that DEEPTYPE narrows down the scope of indirect call targets by 43.11% on average across most benchmarks, reduces runtime overhead by 37.02% on average and consumes less memory compared to TypeDive. A case study in CVE exploit demonstrated that SMLTA is more powerful than MLTA in reducing attack surface and preventing exploits. However, the intrinsic limitation of type-based analysis can still produce false positive targets. We leave it as future work to further improve accuracy through lightweight data-flow analysis.

## Acknowledgment

We thank our shepherd and the anonymous reviewers for their insightful comments. Thanks to Taegy Kim and Kaiming Huang for their suggestions and help. This work is supported in part by National Science Foundation (NSF) under grants CNS-2247652 and CNS-1652790.

## References

- [1] Martín Abadi, Mihai Budiu, Úlfar Erlingsson, and Jay Ligatti. Control-flow integrity. In Proceedings of the 12th ACM Conference on Computer and Communications Security, CCS '05, page 340–353, New York, NY, USA, 2005. Association for Computing Machinery.
- [2] Kevin Backhouse. Cueing up a calculator: an introduction to exploit development on linux. <https://github.blog/2023-12-06-cueing-up-a-calculator-an-introduction-to-exploit-development-on-linux/>, 2023.
- [3] Marcel Böhme, Van-Thuan Pham, Manh-Dung Nguyen, and Abhik Roychoudhury. Directed greybox fuzzing. In Proceedings of the 2017 ACM SIGSAC Conference on Computer and Communications Security, CCS '17, page 2329–2344, New York, NY, USA, 2017. Association for Computing Machinery.
- [4] Peter Boonstoppel, Cristian Cadar, and Dawson Engler. Rwsset: Attacking path explosion in constraint-based test generation. In Proceedings of the Theory and Practice of Software, 14th International Conference on Tools and Algorithms for the Construction and Analysis of Systems, TACAS'08/ETAPS'08, page 351–366, Berlin, Heidelberg, 2008. Springer-Verlag.
- [5] David Brumley and Dawn Song. Privtrans: Automatically partitioning programs for privilege separation. In 13th USENIX Security Symposium (USENIX Security 04), San Diego, CA, August 2004. USENIX Association.
- [6] Nathan Burow, Scott A. Carr, Joseph Nash, Per Larsen, Michael Franz, Stefan Brunthaler, and Mathias Payer. Control-flow integrity: Precision, security, and performance. ACM Comput. Surv., 50(1), apr 2017.
- [7] Cristian Cadar, Daniel Dunbar, and Dawson Engler. Klee: Unassisted and automatic generation of high-coverage tests for complex systems programs. In Proceedings of the 8th USENIX Conference on Operating Systems Design and Implementation, OSDI'08, page 209–224, USA, 2008. USENIX Association.
- [8] Miguel Castro, Manuel Costa, Jean-Philippe Martin, Marcus Peinado, Periklis Akravidis, Austin Donnelly, Paul Barham, and Richard Black. Fast byte-granularity software fault isolation. In Proceedings of the ACM SIGOPS 22nd Symposium on Operating Systems Principles, SOSP '09, page 45–58, New York, NY, USA, 2009. Association for Computing Machinery.
- [9] Hongxu Chen, Yinxing Xue, Yuekang Li, Bihuan Chen, Xiaofei Xie, Xiuheng Wu, and Yang Liu. Hawkeye: Towards a desired directed greybox fuzzer. In Proceedings of the 2018 ACM SIGSAC Conference on Computer and Communications Security, CCS '18, page 2095–2108, New York, NY, USA, 2018. Association for Computing Machinery.
- [10] Vitaly Chipounov, Volodymyr Kuznetsov, and George Candea. S2e: A platform for in-vivo multi-path analysis of software systems. In Proceedings of the Sixteenth International Conference on Architectural Support for Programming Languages and Operating Systems, ASPLOS XVI, page 265–278, New York, NY, USA, 2011. Association for Computing Machinery.
- [11] CVE-2023-43642. <https://cve.mitre.org/cgi-bin/cvename.cgi?name=CVE-2023-43641>, 2023.
- [12] Ren Ding, Chenxiong Qian, Chengyu Song, Bill Harris, Taesoo Kim, and Wenke Lee. Efficient protection of Path-Sensitive control security. In 26th USENIX Security Symposium (USENIX Security 17), pages 131–148, Vancouver, BC, August 2017. USENIX Association.
- [13] Xinyang Ge, Weidong Cui, and Trent Jaeger. Griffin: Guarding control flows using intel processor trace. In Proceedings of the Twenty-Second International Conference on Architectural Support for Programming Languages and Operating Systems, ASPLOS '17, page 585–598, New York, NY, USA, 2017. Association for Computing Machinery.
- [14] Xinyang Ge, Nirupama Talele, Mathias Payer, and Trent Jaeger. Fine-grained control-flow integrity for kernel software. In 2016 IEEE European Symposium on Security and Privacy, pages 179–194, 2016.
- [15] Istvan Haller, Enes Göktas, Elias Athanasopoulos, Georgios Portokalidis, and Herbert Bos. Shrinkwrap: Vtable protection without loose ends. In Proceedings of the 31st Annual Computer Security Applications Conference, ACSAC '15, page 341–350, New York, NY, USA, 2015. Association for Computing Machinery.
- [16] Hong Hu, Chenxiong Qian, Carter Yagemann, Simon Pak Ho Chung, William R. Harris, Taesoo Kim, and Wenke Lee. Enforcing unique code target property for control-flow integrity. In Proceedings of the 2018 ACM SIGSAC Conference on Computer and Communications Security, CCS '18, page 1470–1486, New York, NY, USA, 2018. Association for Computing Machinery.
- [17] Kaiming Huang, Yongzhe Huang, Mathias Payer, Zhiyun Qian, Jack Sampson, Gang Tan, and Trent Jaeger. The taming of the stack: Isolating stack data from memory errors. In Network and Distributed System Security Symposium (NDSS), San Diego, CA, USA, 2022. The Internet Society.
- [18] Yongzhe Huang, Vikram Narayanan, David Detweiler, Kaiming Huang, Gang Tan, Trent Jaeger, and Anton Burtsev. KSplit: Automating device driver isolation. In 16th USENIX Symposium on Operating Systems Design and Implementation (OSDI 22), pages 613–631. USENIX Association, July 2022.
- [19] Kyriakos K. Ispoglou, Bader Albassam, Trent Jaeger, and Mathias Payer. Block oriented programming: Automating data-only attacks. In Proceedings of the 2018 ACM SIGSAC Conference on Computer and Communications Security, CCS '18, page 1868–1882, New York, NY, USA, 2018. Association for Computing Machinery.
- [20] Suman Jana, Yuan Jochen Kang, Samuel Roth, and Baishakhi Ray. Automatically detecting error handling bugs using error specifications. In 25th USENIX Security Symposium (USENIX Security 16), pages 345–362, Austin, TX, August 2016. USENIX Association.
- [21] Dongseok Jang, Zachary Tatlock, and Sorin Lerner. Safedispatch: Securing c++ virtual calls from memory corruption attacks. In Network and Distributed System Security Symposium, 2014.
- [22] Yuan Kang, Baishakhi Ray, and Suman Jana. Apex: Automated inference of error specifications for c apis. In Proceedings of the 31st IEEE/ACM International Conference on Automated Software Engineering, ASE '16, page 472–482, New York, NY, USA, 2016. Association for Computing Machinery.
- [23] Sun Hyoung Kim, Cong Sun, Dongrui Zeng, and Gang Tan. Refining indirect call targets at the binary level. In Network and Distributed System Security Symposium (NDSS), 2021.
- [24] Sun Hyoung Kim, Dongrui Zeng, Cong Sun, and Gang Tan. Binpointer: Towards precise, sound, and scalable binary-level pointer analysis. In Proceedings of the 31st ACM SIGPLAN International Conference on Compiler Construction, CC 2022, page 169–180, New York, NY, USA, 2022. Association for Computing Machinery.
- [25] Zhenpeng Lin, Yueqi Chen, Yuhang Wu, Dongliang Mu, Chensheng Yu, Xinyu Xing, and Kang Li. Grebe: Unveiling exploitation potential for linux kernel bugs. In 2022 IEEE Symposium on Security and Privacy (SP), pages 2078–2095, 2022.



- [26] Shen Liu, Gang Tan, and Trent Jaeger. Ptrsplit: Supporting general pointers in automatic program partitioning. In Proceedings of the 2017 ACM SIGSAC Conference on Computer and Communications Security, CCS '17, page 2359–2371, New York, NY, USA, 2017. Association for Computing Machinery.
- [27] Kangjie Lu and Hong Hu. Where does it go? refining indirect-call targets with multi-layer type analysis. In Proceedings of the 2019 ACM SIGSAC Conference on Computer and Communications Security, CCS '19, page 1867–1881, New York, NY, USA, 2019. Association for Computing Machinery.
- [28] Yandong Mao, Haogang Chen, Dong Zhou, Xi Wang, Nickolai Zeldovich, and M. Frans Kaashoek. Software fault isolation with api integrity and multi-principal modules. In Proceedings of the Twenty-Third ACM Symposium on Operating Systems Principles, SOSP '11, page 115–128, New York, NY, USA, 2011. Association for Computing Machinery.
- [29] Samuel Mergendahl, Nathan Burow, and Nathan Burow. Cross-language attacks. In Network and Distributed System Security Symposium (NDSS), 2022.
- [30] Robin Milner. A theory of type polymorphism in programming. Journal of Computer and System Sciences, 17(3):348–375, 1978.
- [31] Nicholas Nethercote and Julian Seward. Valgrind: a framework for heavyweight dynamic binary instrumentation. SIGPLAN Not., 42(6):89–100, jun 2007.
- [32] Manh-Dung Nguyen, Sébastien Bardin, Richard Bonichon, Roland Groz, and Matthieu Lemerre. Binary-level directed fuzzing for Use-After-Free vulnerabilities. In 23rd International Symposium on Research in Attacks, Intrusions and Defenses (RAID 2020), pages 47–62, San Sebastian, October 2020. USENIX Association.
- [33] Flemming Nielson. The typed lambda-calculus with first-class processes. In Proceedings of the Parallel Architectures and Languages Europe, Volume II: Parallel Languages, PARLE '89, page 357–373, Berlin, Heidelberg, 1989. Springer-Verlag.
- [34] Ben Niu and Gang Tan. Modular control-flow integrity. In Proceedings of the 35th ACM SIGPLAN Conference on Programming Language Design and Implementation, PLDI '14, page 577–587, New York, NY, USA, 2014. Association for Computing Machinery.
- [35] Ben Niu and Gang Tan. Per-input control-flow integrity. In Proceedings of the 22nd ACM SIGSAC Conference on Computer and Communications Security, CCS '15, page 914–926, New York, NY, USA, 2015. Association for Computing Machinery.
- [36] Shankara Pailoor, Andrew Aday, and Suman Jana. MoonShine: Optimizing OS fuzzer seed selection with trace distillation. In 27th USENIX Security Symposium (USENIX Security 18), pages 729–743, Baltimore, MD, August 2018. USENIX Association.
- [37] Jens Palsberg. Type-based analysis and applications. In Proceedings of the 2001 ACM SIGPLAN-SIGSOFT workshop on Program analysis for software tools and engineering, pages 20–27, 2001.
- [38] Eric Pauley, Gang Tan, Danfeng Zhang, and Patrick McDaniel. Performant binary fuzzing without source code using static instrumentation. In 2022 IEEE Conference on Communications and Network Security (CNS), pages 226–235, 2022.
- [39] Hui Peng, Yan Shoshitaishvili, and Mathias Payer. T-fuzz: Fuzzing by program transformation. In 2018 IEEE Symposium on Security and Privacy (SP), pages 697–710, 2018.
- [40] Aravind Prakash, Xunchao Hu, and Heng Yin. vfguard: Strict protection for virtual function calls in cots c++ binaries. In Network and Distributed System Security Symposium, 2015.
- [41] Ryan Roemer, Erik Buchanan, Hovav Shacham, and Stefan Savage. Return-oriented programming: Systems, languages, and applications. ACM Trans. Inf. Syst. Secur., 15(1), mar 2012.
- [42] Konstantin Rubinov, Lucia Rosculete, Tulika Mitra, and Abhik Roychoudhury. Automated partitioning of android applications for trusted execution environments. In Proceedings of the 38th International Conference on Software Engineering, ICSE '16, page 923–934, New York, NY, USA, 2016. Association for Computing Machinery.
- [43] Suman Saha, Jean-Pierre Lozi, Gaël Thomas, Julia L. Lawall, and Gilles Muller. Hector: Detecting resource-release omission faults in error-handling code for systems software. In 2013 43rd Annual IEEE/IFIP International Conference on Dependable Systems and Networks (DSN), pages 1–12, 2013.
- [44] Felix Schuster, Thomas Tendyck, Christopher Liebchen, Lucas Davi, Ahmad-Reza Sadeghi, and Thorsten Holz. Counterfeit object-oriented programming: On the difficulty of preventing code reuse attacks in c++ applications. In 2015 IEEE Symposium on Security and Privacy, pages 745–762, 2015.
- [45] Hovav Shacham. The geometry of innocent flesh on the bone: Return-into-libc without function calls (on the x86). In Proceedings of the 14th ACM Conference on Computer and Communications Security, CCS '07, page 552–561, New York, NY, USA, 2007. Association for Computing Machinery.
- [46] Yan Shoshitaishvili, Ruoyu Wang, Christopher Salls, Nick Stephens, Mario Polino, Audrey Dutcher, John Grosen, Siji Feng, Christophe Hauser, Christopher Kruegel, and Giovanni Vigna. SoK: (State of) The Art of War: Offensive Techniques in Binary Analysis. In IEEE Symposium on Security and Privacy, 2016.
- [47] Mathias Payer Sirus Shahini, Mu Zhang and Robert Ricci. Arvin: Greybox fuzzing using approximate dynamic cfg analysis. In The 18th ACM ASIA Conference on Computer and Communications Security, 2023.
- [48] Yulei Sui and Jingling Xue. Svf: interprocedural static value-flow analysis in llvm. In Proceedings of the 25th international conference on compiler construction, pages 265–266. ACM, 2016.
- [49] Caroline Tice, Tom Roeder, Peter Collingbourne, Stephen Checkoway, Úlfar Erlingsson, Luis Lozano, and Geoff Pike. Enforcing Forward-Edge Control-Flow integrity in GCC & LLVM. In 23rd USENIX Security Symposium (USENIX Security 14), pages 941–955, San Diego, CA, August 2014. USENIX Association.
- [50] David Trabish, Andrea Mattavelli, Noam Rinetzky, and Cristian Cadar. Chopped symbolic execution. In Proceedings of the 40th International Conference on Software Engineering, ICSE '18, page 350–360, New York, NY, USA, 2018. Association for Computing Machinery.
- [51] Victor van der Veen, Dennis Andriess, Enes Göktaş, Ben Gras, Lionel Sambuc, Asia Slowinska, Herbert Bos, and Cristiano Giuffrida. Practical context-sensitive cfi. In Proceedings of the 22nd ACM SIGSAC Conference on Computer and Communications Security, CCS '15, page 927–940, New York, NY, USA, 2015. Association for Computing Machinery.
- [52] Victor van der Veen, Enes Göktaş, Moritz Contag, Andre Pawoloski, Xi Chen, Sanjay Rawat, Herbert Bos, Thorsten Holz, Elias Athanasopoulos, and Cristiano Giuffrida. A tough call: Mitigating advanced code-reuse attacks at the binary level. In 2016 IEEE Symposium on Security and Privacy (SP), pages 934–953, 2016.
- [53] Dennis Volpano and Geoffrey Smith. A type-based approach to program security. In TAPSOFT'97: Theory and Practice of Software Development: 7th International Joint Conference CAAP/FASE Lille, France, April 14–18, 1997 Proceedings 22, pages 607–621. Springer, 1997.
- [54] Whole program LLVM. <https://github.com/travitch/whole-program-llvm>.
- [55] Wikipedia contributors. Address space layout randomization — Wikipedia, the free encyclopedia, 2023. [Online; accessed 3-April-2023].

- [56] Wikipedia contributors. Breadth-first search — Wikipedia, the free encyclopedia, 2023. [Online; accessed 7-October-2023].
- [57] Wikipedia contributors. Virtual method table — Wikipedia, the free encyclopedia, 2023. [Online; accessed 6-October-2023].
- [58] Robert P. Wilson and Monica S. Lam. Efficient context-sensitive pointer analysis for c programs. *SIGPLAN Not.*, 30(6):1–12, jun 1995.
- [59] A.K. Wright and M. Felleisen. A syntactic approach to type soundness. *Information and Computation*, 115(1):38–94, 1994.
- [60] Wei Wu, Yueqi Chen, Xinyu Xing, and Wei Zou. KEPLER: Facilitating control-flow hijacking primitive evaluation for linux kernel vulnerabilities. In *28th USENIX Security Symposium (USENIX Security 19)*, pages 1187–1204, Santa Clara, CA, August 2019. USENIX Association.
- [61] Meng Xu, Chenxiong Qian, Kangjie Lu, Michael Backes, and Taesoo Kim. Precise and scalable detection of double-fetch bugs in os kernels. In *2018 IEEE Symposium on Security and Privacy (SP)*, pages 661–678, 2018.
- [62] Yutian Yang, Wenbo Shen, Xun Xie, Kangjie Lu, Mingsen Wang, Tianyu Zhou, Chenggang Qin, Wang Yu, and Kui Ren. Making memory account accountable: Analyzing and detecting memory missing-account bugs for container platforms. In *Proceedings of the 38th Annual Computer Security Applications Conference, ACSAC '22*, page 869–880, New York, NY, USA, 2022. Association for Computing Machinery.
- [63] Yizhuo Zhai, Yu Hao, Hang Zhang, Daimeng Wang, Chengyu Song, Zhiyun Qian, Mohsen Lesani, Srikanth V. Krishnamurthy, and Paul Yu. Ubitect: A precise and scalable method to detect use-before-initialization bugs in linux kernel. In *Proceedings of the 28th ACM Joint Meeting on European Software Engineering Conference and Symposium on the Foundations of Software Engineering, ESEC/FSE 2020*, page 221–232, New York, NY, USA, 2020. Association for Computing Machinery.
- [64] Chao Zhang, Dawn Song, Scott A. Carr, Mathias Payer, Tongxin Li, Yu Ding, and Chengyu Song. Vtrust: Regaining trust on virtual calls. In *NDSS*, The Internet Society, 2016.
- [65] Chao Zhang, Tao Wei, Zhaofeng Chen, Lei Duan, László Szekeres, Stephen McCamant, Dawn Song, and Wei Zou. Practical control flow integrity and randomization for binary executables. In *2013 IEEE Symposium on Security and Privacy*, pages 559–573, 2013.
- [66] Jinquan Zhang, Pei Wang, and Dinghao Wu. Libsteal: Model extraction attack towards deep learning compilers by reversing dnn binary library. In *18th International Conference on Evaluation of Novel Approaches to Software Engineering (ENASE 2023)*, pages 283–292, 2023.
- [67] Mingwei Zhang and R. Sekar. Control flow integrity for COTS binaries. In *22nd USENIX Security Symposium (USENIX Security 13)*, pages 337–352, Washington, D.C., August 2013. USENIX Association.
- [68] Tong Zhang, Wenbo Shen, Dongyoon Lee, Changhee Jung, Ahmed M. Azab, and Ruowen Wang. PeX: A permission check analysis framework for linux kernel. In *28th USENIX Security Symposium (USENIX Security 19)*, pages 1205–1220, Santa Clara, CA, August 2019. USENIX Association.

## Appendix

### A Multi-Layer Mappings

To efficiently organize and access the collected multi-layer types, we use multi-layer mappings to hierarchically archive them as described in Section 4.2. The question is *how many mappings are sufficient in Type Lookup Maps?* The number should neither be too large to guarantee the performance of DEEPTYPE nor too small to hold the multi-layer types. So, we decide the number of mappings conforming to the multi-layer types in benchmarks.

Table 9 shows the number of multi-layer types with different layer counts. Across all benchmarks, the multi-layer types in them contain at most 8 layers, which means 7-layer mappings are sufficient to record these multi-layer types. Thus, we adopt 7-layer mappings in our implementation. If multi-layer types with more than 8 layers are common in other programs, more mappings can be deployed in DEEPTYPE to supply extra precision in practice.

Programs	Total	<=8 layers	> 8 Layers
binutils	311*	311*	0
sqlite	220	220	0
nginx	101	101	0
httpd	88	88	0
openvpn	43	43	0
proftpd	88	88	0
sshd	46	46	0
linux	5,447	5,447	0

**Table 9: Number of multi-layer types with different layer counts.** 311\* indicates the average of binutils programs.

### B Binutils Test results

Binutils programs consist of similar indirect calls as they utilize shared library function, thus displaying similar results. For someone who is interested in, we provide detailed data for each individual program in Table 10.

Program	DEEPTYPE	DT-weak	TypeDive
addr2line	2.38	2.62	8.60
ar	2.45	2.69	12.73
bfdtest1	2.38	2.62	12.89
bfdtest2	2.38	2.63	12.89
cxxfilt	2.37	2.62	8.64
nm-new	2.48	2.72	13.01
objcopy	2.63	2.87	13.08
objdump	2.95	3.19	11.26
ranlib	2.45	2.69	12.73
readelf	2.29	2.29	2.30
size	2.39	2.64	12.95
strings	2.37	2.62	8.64
strip-new	2.63	2.87	13.08

**Table 10: Average number of targets for each program in binutils.**